

Lattice Mismatch and Interfacial Disorder in Superlattices

D. Neerincx, J.-P. Locquet, L. Stockman and Y. Bruynseraede

Laboratorium voor Vaste Stof-Fysika en Magnetisme, Katholieke Universiteit Leuven, B-3030 Leuven, Belgium

and

Ivan K. Schuller

Physics Department-B019, University of California–San Diego, LaJolla, California 92093, U.S.A.

Received June 18, 1988; accepted in revised form October 11, 1988

Abstract

We have developed a general X-ray diffraction model which enables to investigate interfacial disorder in crystalline/amorphous and crystalline/crystalline multilayers. Using classical structure factor calculations, we simulate the evolution of the diffracted X-ray intensities as a function of the fluctuation amplitude, the superlattice wavelength and the interatomic distances. From experimental X-ray diffraction patterns, the interfacial disorder is extracted as a function of superlattice wavelength for various crystalline/crystalline systems. An enhanced lattice mismatch between the two components gives rise to an increase of interfacial disorder.

The production and investigation of new materials that do not occur naturally is an issue of much current interest. Thin film deposition techniques, such as molecular beam epitaxy and sputtering, are being extensively used to prepare artificially layered structures. Most work to date has been performed on semiconductor and metallic superlattices which are lattice matched [1]. It has been shown that it is possible to achieve superlattice growth of materials with a large lattice mismatch and different crystal symmetry [2], which enables the investigation of the problem of coherence across an interface. Moreover, these superlattices are found to exhibit a series of interesting physical properties [3]. In this work we relate the structural properties of several metallic superlattices to crystal symmetry and lattice mismatch, using a recently developed model for superlattices [4].

Structural properties of superlattices are most easily studied by standard $\theta - 2\theta$ X-ray diffraction techniques [3]. In order to interpret the measured X-ray intensity profiles, structural models have to be developed and the calculated intensities compared to the data. To date, a variety of models for compositionally modulated structures have been calculated. In the sample step model [3] the lattice spacings of the two constituent materials retain their bulk value within each layer, whereas the uniform strain model [5] assumes that one single lattice spacing is maintained throughout all layers. These two models can explain the positions and relative intensities of X-ray peaks of crystalline/crystalline multilayers [5, 12], but cannot account for the observed large peak widths. An even larger discrepancy is found in crystalline/amorphous multilayers [13], where at high 2θ angles only one broad peak is observed, caused by a reduction of the structural coherence length ξ . In realistic models, structural disorder has to be built in as a mechanism to reduce long range coherence.

Most models assume gaussian fluctuations of the modulation wavelength Λ [7, 15] or of the individual layer thicknesses

[11, 13]. A distinction is to be made between *continuous* gaussian fluctuations, which originate from an amorphous interface, and *discrete* gaussian fluctuations resulting from crystalline interfaces. A *discrete* fluctuation distribution with one interatomic distance width has little effect on the high-angle X-ray spectra from crystalline/crystalline multilayers, except for a disappearance of secondary superlattice maxima and a slight reduction in intensity [16]. In contrast, a *continuous* gaussian distribution with the same width leads to the disappearance of all high-angle superlattice peaks. For instance a continuous fluctuations of about 2 Å on the amorphous layer thickness in crystalline/amorphous multilayers explains the observed loss of all superstructure at high angles [13].

Here we present a model for crystalline/crystalline multilayers taking into account continuous gaussian fluctuations only on the interface distance (the distance between two planes of *different* material). We consider a superlattice consisting of M bilayers of N_a planes of material A at distance d_a and with atomic scattering factor f_a , and N_b planes of material B at distance d_b and with atomic scattering factor f_b . We assume each interface distance to be continuous gaussian distributed around an average \bar{a} , conventionally taken to be $(d_a + d_b)/2$, and with distribution width c^{-1} . Using kinematical structure factor calculations [4], the average diffracted intensity (with scattering vector q perpendicular to the layers), is given as:

$$I(q) = M(A^2 + B^2 + 2AB \exp(-q^2/4c^2) \cos(q\Lambda/2)) \\ + 2 \sum_{m=1}^{M-1} (M-m) \{ (A^2 + B^2) \exp(-2mq^2/4c^2) \\ \times \cos(2mq\Lambda/2) + AB (\exp(-(2m+1)q^2/4c^2) \\ \times \cos((2m+1)q\Lambda/2) + \exp(-(2m-1)q^2/4c^2) \\ \times \cos((2m-1)q\Lambda/2)) \}$$

with

$$A = f_a \frac{\sin(N_a q d_a / 2)}{\sin(q d_a / 2)}$$

$$B = f_b \frac{\sin(N_b q d_b / 2)}{\sin(q d_b / 2)}$$

$$\Lambda = (N_a - 1)d_a + (N_b - 1)d_b + 2\bar{a}$$

For $c^{-1} = 0$, this equation reduces to the simple step model, while for $f_b = 0$, it reduces to the crystalline/amor-

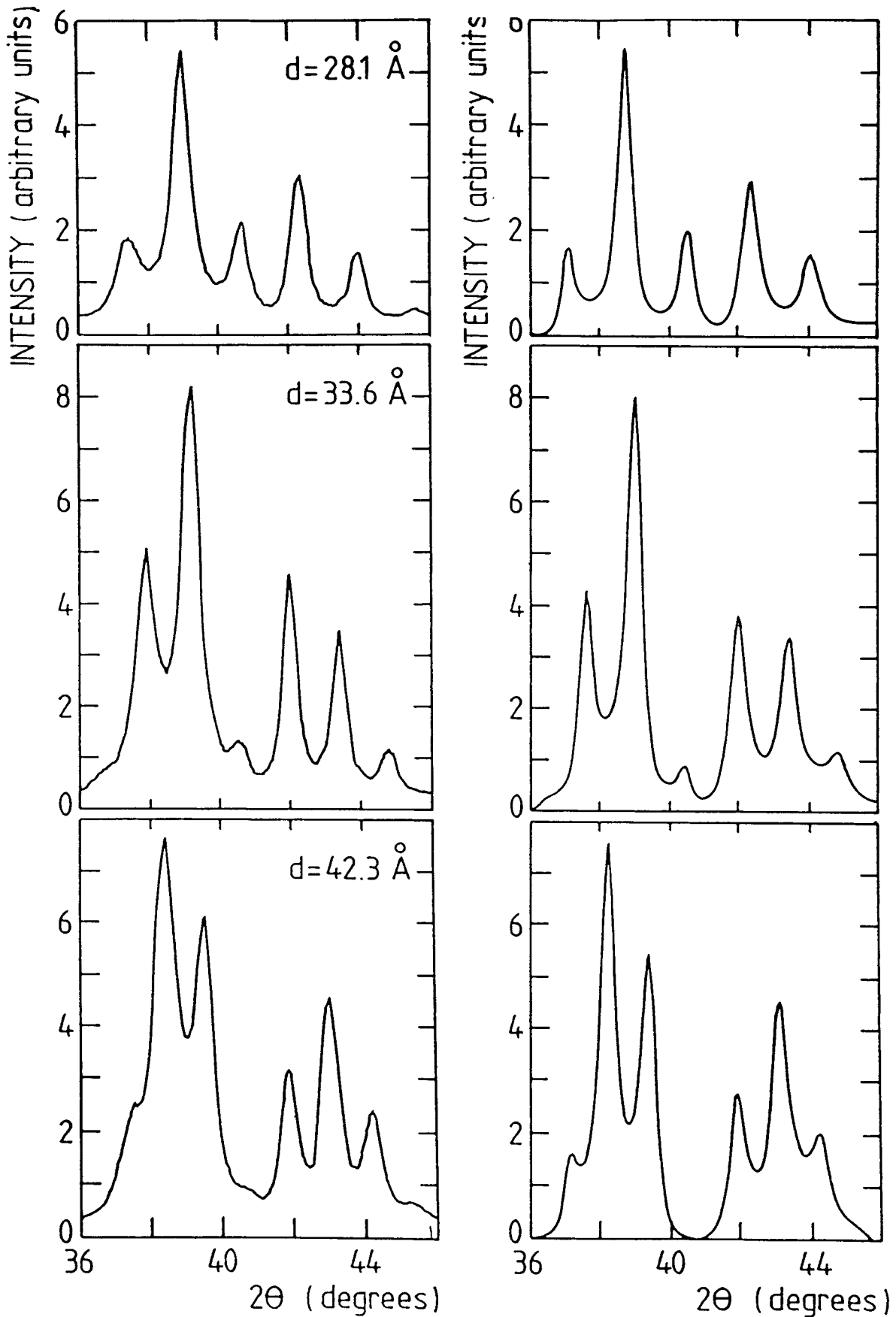


Fig. 1. Comparison between experimental (a) and calculated (b) X-ray spectra from Nb/Cu superlattices for several Λ . The Nb and Cu layer thicknesses are equal and denoted by d . The FWHM of the calculated spectra are 0.15 degrees smaller than the FWHM of the experimental spectra due to instrumental broadening.

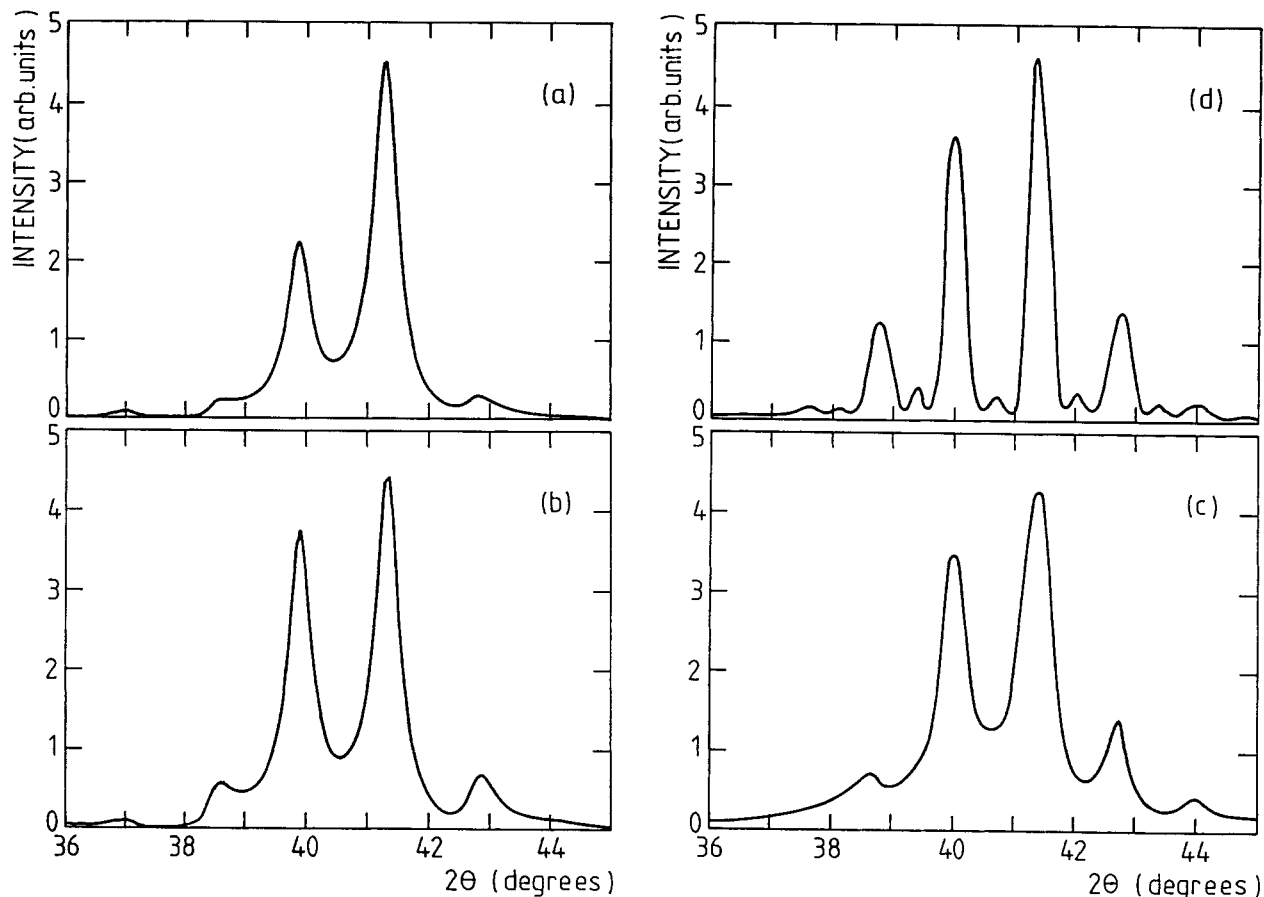


Fig. 2. Calculation of a Mo (35.6 Å)/V (29.9 Å) superlattice, (a) with bulk lattice spacings ($d_{\text{Mo}} = 2.227 \text{ \AA}$, $d_{\text{V}} = 2.135 \text{ \AA}$) and (b) with strained lattice spacings ($d_{\text{Mo}} = 2.237 \text{ \AA}$, $d_{\text{V}} = 2.115 \text{ \AA}$). The experimental data are shown in (c) and the fit using Ariosa's [19] strain profile in (d).

phous case with continuous fluctuations on the amorphous layer thickness [13].

Figure 1 presents measured and calculated high-angle X-ray spectra for equal layer Nb/Cu [2] ($d_{\text{Nb}} = 2.326 \text{ \AA}$, $d_{\text{Cu}} = 2.084 \text{ \AA}$) for different modulation wavelengths Λ and including the usual polarization, Lorentz, Debye-Waller, atomic scattering factors and in-plane densities. The excellent agreement implies that continuous interfacial disorder can account for the large peak widths, resulting in a reduced long-range coherence. This model enables to investigate the amount of interfacial disorder present in several crystalline/crystalline superlattice systems. Since continuous interfacial disorder is expected to be the main disordering mechanism in superlattices with a large lattice mismatch, we studied Nb/Cu [2, 6], Mo/Ni [12], Pd/Au [7], Pb/Ag [8, 9], Fe/V [11], in which the lattice mismatch ($(d_a - d_b)/\text{Max}\{d_a, d_b\}$) is at least 4%. In all these systems mutual interdiffusion, which is not accounted for in our model, is expected to be negligible, because they do not form solid solutions in their thermodynamic phase diagram.

In order to study the influence of coherency strains on the diffracted intensity profile and on the X-ray coherence length, we performed a fit of a Mo/V [19] (lattice mismatch 4.1%) X-ray spectrum using our model, assuming bulk lattice spacings ($d_{\text{Mo}} = 2.227 \text{ \AA}$, $d_{\text{V}} = 2.135 \text{ \AA}$, $c^{-1} = 0.5 \text{ \AA}$, $\bar{a} = 2.181 \text{ \AA}$) (Fig. 2a) and uniformly strained lattice spacings ($d_{\text{Mo}} = 2.237 \text{ \AA}$, $d_{\text{V}} = 2.115 \text{ \AA}$, $c^{-1} = 0.5 \text{ \AA}$, $\bar{a} = 2.176 \text{ \AA}$) (Fig. 2b). The agreement of Fig. 2b with the experimental data (Fig. 2c) shows the importance of both strain and interfacial disorder in Mo/V superlattices. However, the main effect of strain is to change relative peak intensities, since

coherence lengths, as extracted from the full width at half maximum of the X-ray peaks (FWHM), agree within 0.2% for the strained and unstrained superlattice. Therefore, our model, including interfacial disorder fits better to the experimental data than Ariosa's [19] strain profile (Fig. 2d), where no interfacial disorder was included.

In order to investigate systematically the amount of interfacial disorder (distribution width c^{-1}), the model is characterized by the reduction of the X-ray coherence length ξ by

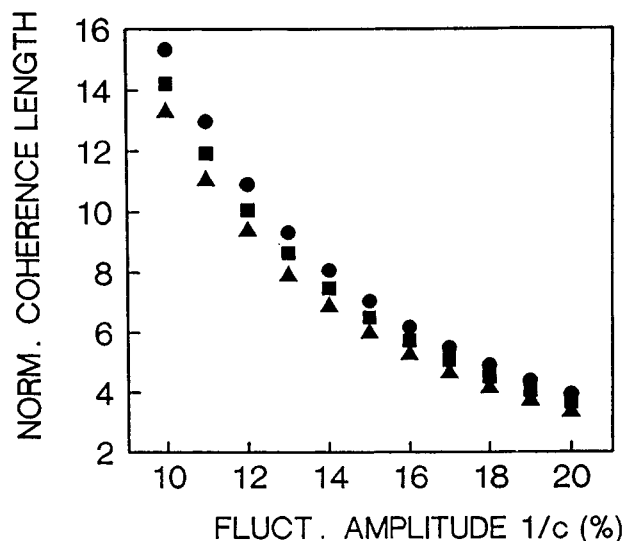


Fig. 3. Dependence of the X-ray coherence length ξ , extracted from the FWHM of calculated Nb (30.2 Å)/Cu (22.9 Å) spectra as a function of fluctuation amplitude c^{-1} , expressed as a percentage of the average interface distance \bar{a} , for three peak positions (38.93 (●), 40.70 (■), 42.47 (▲) degrees 2θ).

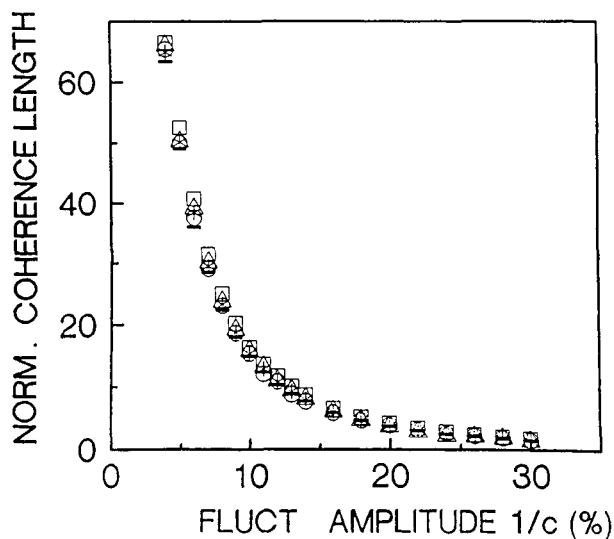


Fig. 4. Normalized coherence length ξ/Λ versus fluctuation amplitude c^{-1} , expressed as a percentage of the average interface distance \bar{a} , showing a universal behaviour for all superlattice systems (Nb/Cu (○), Mo/Ni (Δ), Pb/Ag (□), Pd/Au (*), Fe/V (—)).

the interfacial disorder. We calculated the X-ray pattern for different c^{-1} values and extracted ξ from the FWHM of the X-ray peaks using Scherrer's equation:

$$\xi = \frac{0.9\lambda_x}{B \cos \theta_b}$$

where λ_x is the X-ray wavelength, θ_b the Bragg angle and B the FWHM in 2θ radians. Care should be taken when a comparison is made between different modulation wavelengths and different systems, since simulations show that ξ is dependent on 2θ (and hence on $d = n\lambda_x/2 \sin \theta$ via Bragg's law). Figure 3 shows the coherence length as a function of c^{-1} , extracted from three peaks in the calculated spectrum of Nb (27.9 Å)/Cu (27.1 Å). ξ gradually increases with decreasing angle 2θ and therefore, in all calculations, ξ was determined from peaks in a small angular range.

Figure 4 shows the normalized coherence length ξ/Λ as a function of c^{-1} , expressed as a percentage of the average interface distance \bar{a} for several superlattices, assuming bulk lattice spacings. This curve is a complete characterization of

the model and is universal as expected since we are using normalized units. Figure 4 allows a direct determination of the fluctuation amplitude c^{-1} in a superlattice, with ξ extracted from the experimental FWHM, corrected for an estimated instrumental broadening of 0.15 degrees. This method was applied for multilayers with large lattice mismatch and different crystal symmetry. Figure 5a shows the fluctuation amplitude for two b.c.c./f.c.c. superlattices (Nb/Cu, Mo/Ni), while Fig. 5b shows the result for two f.c.c./f.c.c. (Pd/Au, Pb/Ag) and one b.c.c./b.c.c. (Fe/V) system.

An enhanced lattice mismatch clearly gives rise to a large amount of interfacial disorder. Although the results are quite similar for all crystal symmetries, b.c.c./f.c.c. superlattices show a sudden uprise of c^{-1} at the smallest Λ . This high interfacial disorder is an indication of the loss of texture and non-continuous layer growth observed in b.c.c./f.c.c. superlattices at small Λ [2, 6, 10, 12]. The modulation wavelength below which loss of texture occurs, is approximately 15 Å for Nb/Cu and Mo/Ni superlattices, while for Nb/Al superlattices it is much larger (50 Å) due to substantial interdiffusion.

For all systems, the distribution width c^{-1} at small Λ approaches the absolute value of the difference in lattice spacing. In this Λ -region, the lattice mismatch can account for all observed interfacial disorder. This purely geometrical argument cannot explain the increase in disorder at higher Λ , indicating that a supplementary disordering mechanism becomes important with increasing Λ . Continuous interfacial disorder can also be caused by misfit dislocations, as described by the formalism used by Hilliard [20]. He showed that the dislocation energy (the energy needed to introduce a dislocation at the interface) is *inversely proportional* to Λ , while the coherency strain energy (the energy needed to impose one lattice spacing in the plane of the layers) is *proportional* to Λ . Therefore strains are energetically favorable at small Λ , dislocations at high Λ . The fluctuation amplitude c^{-1} represents the interfacial dislocation density, in addition to the geometrical disorder caused by the lattice mismatch (since strains are shown to be of no importance in the systems under consideration here). The increase of c^{-1} with increasing Λ can then be completely attributed to the increase of the number of misfit dislocations present at the interface.

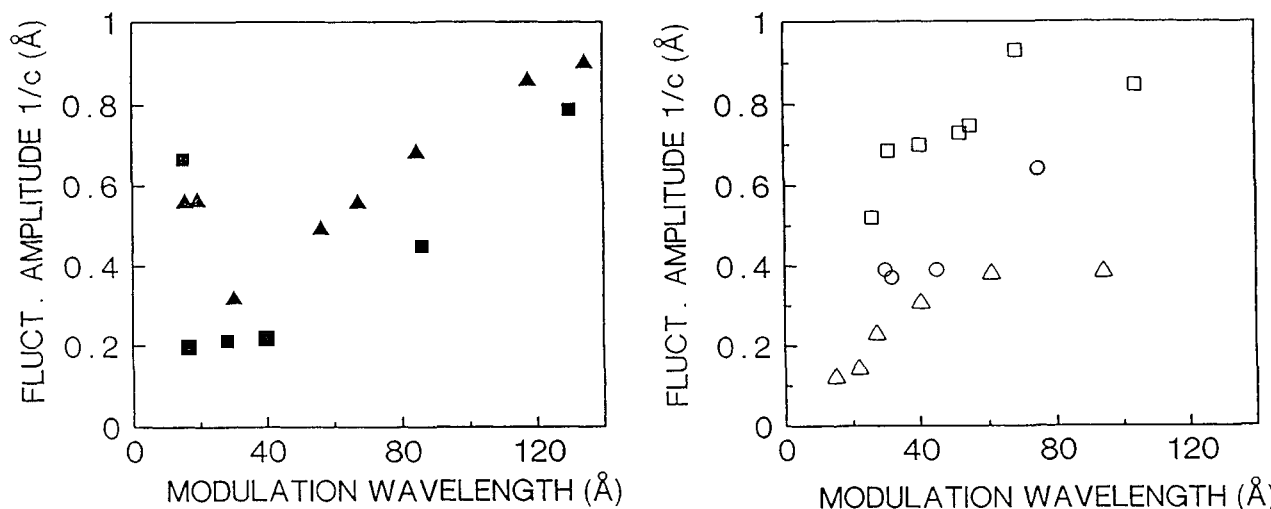


Fig. 5. Fluctuation amplitude c^{-1} versus modulation wavelength Λ for (a) b.c.c./f.c.c. (Nb/Cu (▲, lattice mismatch 10.4% = 0.24 Å), Mo/Ni (■, lattice mismatch 8.56% = 0.19 Å)), (b) f.c.c./f.c.c. (Pd/Au (Δ, lattice mismatch 4.63% = 0.11 Å), Pb/Ag (□, lattice mismatch 17.53% = 0.5 Å)) and b.c.c./b.c.c. (Fe/V (○, lattice mismatch 5.68% = 0.12 Å)) superlattices.

In summary, we presented a structural model for crystal-line/crystalline multilayers which enables to investigate continuous interfacial disorder for several superlattice systems. This interfacial disorder increases with increasing lattice mismatch and can be attributed to the geometrical disorder caused by this lattice mismatch, and the presence of misfit dislocations. The observed increase of the disorder with increasing Λ is then explained by the increase of interfacial dislocation density.

Acknowledgements

This work was supported by the Belgian Inter-University Institute for Nuclear Sciences (I.I.K.W.), the Belgian Inter-University Attraction Poles (I.U.A.P.) programme and the U.S. Department of Energy, under contract number DE-FG03-87ER45332 (at U.C.S.D.). International Travel was provided by NATO grant number RG85-0695 and the Belgian National Fund for Scientific Research (N.F.W.O.). D. Neerincx is a Research Assistant of the N.F.W.O. and J.-P. Locquet is a Research Fellow of the I.I.K.W.

References

1. For an overview, see Gossard, A. C., *Thin Solid Films* **57**, 3 (1979).
2. Schuller, I. K., *Phys. Rev. Lett.* **44**, 1597 (1980).
3. For an overview, see "Synthetic Modulated Structures" (Edited by L. L. Chang and B. C. Giessen) Academic Press, New York (1985).
4. Locquet, J.-P., Neerincx, D., Sevenhans, W., Bruynseraede, Y., Homma, H. and Schuller, I. K., to be published in *Materials Research Society Symposia Proceedings Vol. D103* (Edited by T. W. Barbee, Jr., F. Spaepen and L. Greer) (1988).
5. Segmüller, A. and Blakeslee, A. E., *J. Appl. Cryst.* **6**, 19 (1973).
6. Lowe, W. P., Barbee, T. W., Jr., Geballe, T. H. and McWhan, D. B., *Phys. Rev.* **B24**, 6193 (1981).
7. Carcia, P. F. and Suna, A., *J. Appl. Phys.* **54**, 2000 (1983).
8. Jalochowski, M., *Thin Solid Films* **101**, 285 (1983).
9. Jalochowski, M. and Mikolajczak, P., *J. Phys.* **F13**, 1973 (1983).
10. McWhan, D. B., Gurvitch, M., Rowell, J. M. and Walker, L. R., *J. Appl. Phys.* **54**, 3886 (1983).
11. Endoh, Y., Kawaguchi, K., Hosoito, N., Shinjo, T., Takada, T., Fujii, Y. and Ohnishi, T., *J. Phys. Soc. Japan* **53**, 3481 (1984).
12. M. R. Kahn, Chun, C. S. L., Felcher, G. P., Grimsditch, M., Kueny, A., Falco, C. M. and Schuller, I. K., *Phys. Rev.* **B27**, 7186 (1983).
13. Sevenhans, W., Gijs, M., Bruynseraede, Y., Homma, H. and Schuller, I. K., *Phys. Rev.* **B34**, 5955 (1986).
14. Fuji, Y., Ohnishi, T., Ishihara, T., Yamada, Y., Kawaguchi, K., Nakayama, N. and Shinjo, T., *J. Phys. Soc. Japan* **25**, 552 (1986).
15. Nakayama, N., Takahashi, K., Shinjo, T., Takada, T. and Ichinose, H., *Jap. J. Appl. Phys.* **25**, 552 (1986).
16. Clemens, B. M. and Gay, J. G., *Phys. Rev.* **B35**, 9337 (1987).
17. Gyorgy, E. M., McWhan, D. B., Dillon, J. F., Jr., Walker, L. R. and Waszczak, J. V., *Phys. Rev.* **B25**, 6739 (1982).
18. Durbin, S. M., Cunningham, J. E. and Flynn, C. P., *J. Phys.* **F12**, L75 (1982).
19. Ariosa, D., Fischer, Ø., Karkut, M. G. and Triscone, J.-M., *Phys. Rev.* **B37**, 2415 (1988).
20. Hilliard, J. E., in "Modulated Structures" (Edited by J. M. Cowley, J. B. Cohen, M. B. Salamon and B. J. Wuensch) *A.I.P. Conf. Proc.* **53**, 407 (1979).